Atmospheric
Chemistry
and Physics
Discussions

Open Access

Organic nitrate aerosol formation via NO$_3$ + BVOC in the Southeastern US

B. R. Ayres[1], H. M. Allen[1,2], D. C. Draper[1,3], S. S. Brown[4], R. J. Wild[4], J. L. Jimenez[5,6], D. A. Day[5,6], P. Campuzano-Jost[5,6], W. Hu[5,6], J. de Gouw[5,6], A. Koss[5,6], R. C. Cohen[7], K. C. Duffey[7], P. Romer[7], K. Baumann[8], E. Edgerton[8], S. Takahama[9], J. A. Thornton[10], B. H. Lee[10], F. D. Lopez-Hilfiker[10], C. Mohr[10,11], A. H. Goldstein[12], K. Olson[12], and J. L. Fry[1]

[1]Department of Chemistry, Reed College, Portland, OR, USA
[2]Division of Chemistry and Chemical Engineering, California Institute of Technology, Pasadena, CA, USA
[3]Department of Chemistry, University of California, Irvine, CA, USA
[4]Earth System Research Laboratory, National Oceanic and Atmospheric Administration, Boulder, CO, USA
[5]Cooperative Institute for Research in Environmental Sciences, University of Colorado, Boulder, Colorado, USA
[6]Department of Chemistry and Biochemistry, University of Colorado, Boulder, CO, USA
[7]Department of Chemistry, University of California at Berkeley, CA, USA
[8]Applied Research Associates, Inc., Research Triangle Park, NC, USA

ACPD

15, 16235–16272, 2015

Organic nitrate aerosol formation in the southeastern US

B. R. Ayres et al.

Title Page

Abstract | Introduction

Conclusions | References

Tables | Figures

◄ | ►

◄ | ►

Back | Close

Full Screen / Esc

Printer-friendly Version

Interactive Discussion

[9]Department of Environmental Engineering, École polytechnique fédérale de Lausanne (EPFL), Switzerland
[10]Department of Atmospheric Sciences, University of Washington, Seattle, WA, USA
[11]Karlsruhe Institute of Technology, Karlsruhe, Germany
[12]Department of Environmental Science, Policy, and Management, University of California, Berkeley, CA, USA

Correspondence to: J. L. Fry (fry@reed.edu)

Title Page

Abstract | Introduction

Conclusions | References

Tables | Figures

◄ | ►►

◄ | ►

Back | Close

Full Screen / Esc

Printer-friendly Version

Interactive Discussion

Abstract

Gas- and aerosol-phase measurements of oxidants, biogenic volatile organic compounds (BVOC) and organic nitrates made during the Southern Oxidant and Aerosol Study (SOAS campaign, Summer 2013) in central Alabama show that nitrate radical (NO$_3$) reaction with monoterpenes leads to significant secondary aerosol formation. Cumulative losses of NO$_3$ to terpenes are calculated and correlated to gas and aerosol organic nitrate concentrations made during the campaign. Correlation of NO$_3$ radical consumption to organic nitrate aerosol as measured by Aerosol Mass Spectrometry (AMS) and Thermal Dissociation – Laser Induced Fluorescence (TD-LIF) suggests a range of molar yield of aerosol phase monoterpene nitrates of 23–44 %. Compounds observed via chemical ionization mass spectrometry (CIMS) are correlated to predicted nitrate loss to terpenes and show C$_{10}$H$_{17}$NO$_5$, likely a hydroperoxy nitrate, is a major nitrate oxidized terpene product being incorporated into aerosols. The comparable isoprene product C$_5$H$_9$NO$_5$ was observed to contribute less than 0.5 % of the total organic nitrate in the aerosol-phase and correlations show that it is principally a gas-phase product from nitrate oxidation of isoprene. Organic nitrates comprise between 30 and 45 % of the NO$_y$ budget during SOAS. Inorganic nitrates were also monitored and showed that during incidents of increased coarse-mode mineral dust, HNO$_3$ uptake produced nitrate aerosol mass loading comparable to that of organic nitrate produced via NO$_3$ + BVOC.

1 Introduction

Secondary Organic Aerosol (SOA), formed from the oxidation of volatile organic compounds (VOCs) by ozone (O$_3$), hydroxyl radical (OH), or nitrate radical (NO$_3$), affects visibility as well as regional and global radiative climate forcing (Bellouin et al., 2011; Feng and Penner, 2007; Goldstein et al., 2009; Myhre et al., 2013). SOA is also a source for significant risk factors for pulmonary and cardiac disorders (Nel, 2005;

Pope and Dockery, 2006). Organic aerosol (OA) contributes a large fraction of the total tropospheric submicron particulate matter (PM, De Gouw, 2005; Heald et al., 2005; Zhang et al., 2007). Biogenic volatile organic compounds (BVOC) are dominant precursors in SOA formation (Goldstein and Galbally, 2007; Spracklen et al., 2011). SOA is a significant fraction of total aerosol mass in the southeastern US (predicted to be 80–90 % of the organic aerosol load, Ahmadov et al., 2012; Stocker et al., 2013). Understanding the interaction of anthropogenic pollutants with BVOC is vital to improving our understanding of the human impact on SOA formation (Carlton et al., 2010; Spracklen et al., 2011) in order to improve model parameterizations of these processes as well as reduce uncertainties on the radiative forcing of climate change (Stocker et al., 2013).

Nitrogen oxides ($NO_x = NO + NO_2$), common byproducts of combustion, are linked to aerosol formation in the troposphere via daytime and nighttime oxidation mechanisms (Rollins et al., 2012). Total reactive nitrogen, NO_y, consists of NO_x, as well as NO_x reaction products, including NO_3, HNO_3, HONO, alkyl nitrates, peroxynitrates and other particulate nitrates. Alkyl nitrates produced from oxidation of VOC have been found to be related to tropospheric ozone generation (Chameides, 1978) as well as form SOA via low-volatility products (Hallquist et al., 2009). Oxidation of NO_x can also produce *inorganic* nitrate aerosol via heterogeneous uptake of nitric acid (HNO_3) onto mineral or sea salt aerosols (Vlasenko et al., 2006) and via co-partitioning with ammonia to form semi-volatile NH_4NO_3 (Lee et al., 2008).

NO_3 has been found to be an effective nocturnal oxidizer of BVOC (Atkinson and Arey, 2003, 1998; Calogirou et al., 1999; Winer et al., 1984). NO_3 oxidation is especially reactive towards unsaturated, non-aromatic hydrocarbons of which BVOC are major global constituents. NO_3 is less reactive towards aromatic compounds and saturated hydrocarbons, which are abundant in anthropogenic VOCs. Nitrate oxidation of some BVOC compounds, such as β-pinene, have been shown to lead to rapid production of SOA in laboratory experiments with high yields (Griffin et al., 1999; Jimenez et al., 2009; Zhang et al., 2007; Hallquist et al., 2009; Fry et al., 2011, 2009; Boyd et al., 2015). Analysis of previous field studies have characterized the loss of NO_3 to its major

Organic nitrate aerosol formation in the southeastern US

B. R. Ayres et al.

|◀ | ▶|

◀ | ▶

Back | Close

Full Screen / Esc

Printer-friendly Version

Interactive Discussion

daytime sinks, including reaction with NO and photolysis, as well as its loss to BVOC during both daytime and nighttime (Aldener et al., 2006; Brown et al., 2005).

Nitrogen-containing oxidation products include alkyl nitrates ($RONO_2$), peroxynitrates (RO_2NO_2) and nitric acid (HNO_3) (Brown and Stutz, 2012; Perring et al., 2013),

5 all of which may partition to the aerosol-phase and contribute to SOA (via direct reaction or catalysis) (Kroll and Seinfeld, 2008). Ambient concentrations of alkyl nitrates and peroxynitrates can be quantified using laser-induced fluorescence (Day et al., 2002; Rollins et al., 2010) and mass spectrometry methods (Bahreini et al., 2008; Farmer et al., 2010; Beaver et al., 2012). Ions and acids (i.e. HNO_3) can be quantified using

10 ion chromatography (IC, Makkonen et al., 2012; Trebs et al., 2004). The combination of these instruments, as well as others discussed below, allow for the determination of a total ambient oxidized nitrogen (NO_y) budget, which also supports in the interpretation of the importance of nitrogen oxides in SOA formation.

The 2013 SOAS campaign was a comprehensive field intensive in central Alabama in

15 which concentrations of oxidants, BVOC and aerosol were measured with a particular focus on understanding the effects of anthropogenic pollution on SOA formation. The site was chosen due to its high biogenic VOC emissions as well as its relative distance from anthropogenic pollution (Fig. 1). Alabama is home to a number of power plant facilities that are large point sources of NO_x capable of being carried long distances.

20 Alabama's non-interstate roadways also produce large emissions of NO_x, though a majority of the emissions come from urban areas. Although the NO_x emissions have been steadily dropping since 1998, they are still substantial (2.70 million tons in reported for the southeastern states 1999 to 1.75 million tons in 2008, Blanchard et al., 2013). Frequent controlled biomass burning events (crop burning, Crutzen and Andreae, 1990),

25 as well as vehicular sources (Dallmann et al., 2012) also contribute to local NO_x emissions and PM concentrations (a full analysis of contributions can be found at the EPA National Emissions Inventory,http://www.epa.gov/ttn/chief/net/2011inventory.html).

Lee et al. (2015) describe the observation of particle-phase C_{10} organic nitrate concentrations peaking at night during SOAS, consistent with high SOA yield from

NO_3 + monoterpenes. Observed C_{10} organic nitrates include many highly oxidized molecules, suggesting that substantial additional oxidation beyond the first-generation hydroxynitrates occurs. In this paper, we use the initial products ($C_{10}H_{17}NO_5$), as well as total aerosol phase organic nitrates, to track NO_3 radical contributions to SOA formation. We analyze the role of NO_3 oxidation of BVOC both at night and during the day. Nitrate sinks have been determined for all measured BVOC compounds and correlations of observed alkyl nitrate products vs. these calculated loss rates are discussed.

In the present study, we investigate the production of SOA species from NO_3 reaction with monoterpenes. NO_3 loss to BVOC is calculated and compared to AMS and TD-LIF measurements of aerosol organic nitrates. We compare this to an alternate fate of NO_x, heterogeneous HNO_3 uptake to produce inorganic nitrate aerosol, which is considered in detail in a second paper (Allen et al., 2015). Both pathways from NO_x to nitrate aerosol shown in Scheme 1 produce substantial aerosol at various times in the southeastern US.

2   Experimental

Measurements for the SOAS campaign took place near the Talladega National Forest, 6 miles southwest of Brent, AL (32.9029° N, 87.2497° W), from 1 June–15 July 2013. The forest covers 157 000 acres to the northwest and southeast of Centerville, AL. Figure 1 shows a map of the site location as well as nearby point sources of anthropogenic NO_x and SO_2. The site is in a rural area representative of the transitional nature between the lower coastal plain and Appalachian highlands (Das and Aneja, 2003). Measured wind directions varied allowing for periods of urban influence from sources of anthropogenic emissions located near the sampling site, including the cities of Montgomery, Birmingham, Mobile and Tuscaloosa (Hidy et al., 2014). The closest large anthropogenic NO_x emission point sources are the Alabama Power Company Gaston Plant located near Birmingham and the Green County Power Plant southwest of Tuscaloosa (EPA Air Markets Program 2013). BVOC emissions are dominated by

isoprene, α-pinene, β-pinene, and limonene (Supplement Fig. S1, Stroud et al., 2002; Goldan et al., 1995).

Two cavity ringdown spectrometers (CRDS) were used to determine ambient mixing ratios of NO_x, O_3, NO_y, NO_3 and N_2O_5 (Wild et al., 2014; Wagner et al., 2011). CRDS is a high sensitivity optical absorption method based on the decay time constant for light from an optical cavity composed of two high reflectivity mirrors. NO_2 is measured using its optical absorption at 405 nm in one channel, and O_3, NO and total NO_y are quantitatively converted to NO_2 and measured simultaneously by 405 nm absorption on three additional channels. NO_3 is measured at its characteristic strong absorption band at 662 nm. N_2O_5 is quantitatively converted to NO_3 by thermal dissociation and detected in a second 662 nm channel.

Thermal Dissociation Laser-Induced Fluorescence (TD-LIF) (Day et al., 2002; Farmer et al., 2010; Rollins et al., 2010) was used to measure total alkyl nitrates (ΣANs), total peroxy nitrates (ΣPNs) and aerosol phase ΣANs (Rollins et al., 2012). High-resolution time-of-flight aerosol mass spectrometry (HR-ToF-AMS, hereafter AMS, DeCarlo et al., 2006) was used to measure submicron organic and inorganic nitrate aerosol composition (Fry et al., 2013). TD-LIF and AMS were both used to analyze aerosol organic nitrate concentration. These measurements correlate well to one another, but the magnitudes differ by a factor of approximately 2 for unknown reasons, with TD-LIF being larger than AMS. A high-resolution time-of-flight chemical ionization mass spectrometer (HR-ToF-CIMS, hereafter CIMS, Bertram et al., 2011; Yatavelli et al., 2012) was used to identify specific organic nitrate product ions, specifically monoterpene (Eddingsaas et al., 2012) and isoprene products (Crounse et al., 2013, 2006; Beaver et al., 2012). The CIMS employed a Filter Inlet for Gas and Aerosol (FIGAERO) to separate aerosol and gas species (Lopez-Hilfiker et al., 2014) and was equipped with a high-resolution time-of-flight mass spectrometer capable of resolving ions with different elemental formulae at common nominal m/z.

On-line cryostat-Gas Chromatography-Mass Spectrometer (GC-MS) was used to measure mixing ratios of gas-phase BVOC species (Goldan et al., 2004; Gilman et al.,

2010). Surface area concentration was calculated from number distribution measurements of a hygroscopicity scanning mobility particle sizer (SMPS)/optical particle sizer (OPS) similar to a Dry-Ambient Aerosol Size Spectrometer (Stanier et al., 2004). Boundary layer height was measured using a CHM 15k-Nimbus and method employs photon counting of back-scattered pulse of near-IR light (1064 nm) via LIDAR principle. A Metrohm Monitor for Aerosols and Gases in Ambient Air (MARGA, Makkonen et al., 2012; Trebs et al., 2004), which is a combination wet-rotating denuder/ion chromatogram, measured inorganic ion concentrations at 1 h time resolution in both the aerosol- and gas-phases.

Site infrastructure consisted of a 65-foot tower, with the top platform set above the canopy height for sampling, and seven trailers located in a field 90 m south of the tower. The tower instruments used for this analysis consisted of the two CRDS, TD-LIF and a cryostat GC-MS. The field trailers contained the AMS, SMPS, APS, CIMS and MARGA.

3   Results

3.1   Organic NO_x sink: NO_3 + BVOC production of organic nitrate SOA

During the SOAS campaign, we monitored reactant and product species indicative of NO_3 + BVOC, which may partition into the aerosol-phase and consequently serve as a source of first generation SOA. NO_3 reaction with biogenic alkenes forms organic nitrates.

$$NO_3 + BVOC \rightarrow RONO_2 + \text{other products} \tag{R1}$$
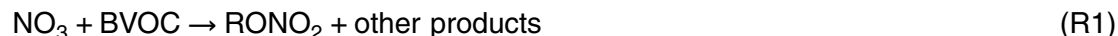
NO_3 and N_2O_5 (which exists in equilibrium with NO_2 + NO_3) in the region were consistently low during the campaign. The result of this was that NO_3 was below the detection limit of the cavity ringdown instrument for the entire campaign. Calculated steady-state N_2O_5 was validated against observed measurements (see below) and NO_3 predicted

from the steady-state approximation was used for all calculations involving NO_3 radical mixing ratios. Using the rate constant for $NO_2 + O_3$ (Table 1), we can calculate the production rate of the nitrate radical ($P(NO_3)$, Eq. 1)

$$P(NO_3) = k_{O_3+NO_2}[O_3][NO_2] \tag{1}$$

The losses of NO_3 to reactions with individual BVOC, NO and modeled photolysis (j_{NO_3} modeled for clear sky from MCM, Saunders et al., 2003) can then be used to calculate the total loss rates, and therefore steady-state lifetime of NO_3 (Eq. 2). Loss of NO_3 through formation and heterogeneous uptake of N_2O_5 is neglected in Eq. (2) because it was negligible relative to NO_3 reactions with BVOC.

$$\tau(NO_3) = \frac{1}{\left(\sum_i k_{NO_3+BVOC_i}[BVOC]_i + k_{NO_3+NO}[NO] + j_{NO_3} \right)} \tag{2}$$

j_{NO_3} values wer adjusted for cloud cover by taking measured solar radiation values (Atmospheric Research and Analysis, Inc., $W\,m^{-2}$) and normalizing their peak values to those of the modeled photolysis data. Peak modeled j_{NO_3} values were typically $0.175\,s^{-1}$ for clear sky at the daily solar maximum.

Using Eqs. (1) and (2), a steady-state predicted NO_3 mixing ratio ($NO_{3,SS}$) can be calculated (Eq. 3):

$$[NO_3]_{SS} = \frac{P(NO_3)}{\tau(NO_3)^{-1}} \tag{3}$$

$NO_{3,SS}$ can then be used to calculate steady-state predicted N_2O_5 from the N_2O_5 equilibrium (Table 1) and measured NO_2 (Eq. 4)

$$[N_2O_5]_{SS} = K_{eq}[NO_2][NO_3]_{SS} \tag{4}$$

where K_{eq} is $2.7 \times 10^{-27} \exp^{(11\,000/T)}$ cm^3 molecule^{-1} s^{-1} (Sander et al., 2011, see Table 1). Comparison of the predicted N_2O_5 to the measured N_2O_5 mixing ratios for the campaign demonstrates that both timing and magnitude of predicted N_2O_5 peaks match observations (Fig. S2) . Since predicted steady-state N_2O_5 tracked observations when the latter were available, $NO_{3,SS}$ is hereafter used as the best estimate of NO_3 to calculate production rates of BVOC-nitrate products.

A substantial fraction (30–45 %) of the NO_y budget is comprised of organic nitrates (ΣAN + ΣPN, Fig. S3). Measurements of gas phase and aerosol phase alkyl nitrates 28 June–July 15 show that a substantial fraction of the organic nitrates are in the aerosol-phase (30 % when aerosol phase AMS is compared to TD-LIF's ΣAN vs. 80 % when using only TD-LIF for the comparison, at 5 a.m. CDT) when total ΣAN concentration builds up (Figs. 2 and 3). The average diurnal cycle shown in Fig. 3 also shows that TD-LIF measured ΣANs are almost completely in the aerosol phase at night, but only about 50 % in the aerosol phase during the day. During peaks in $NO_{3,SS}$, we see corresponding spikes in the ΣAN concentrations, all of which occur during nighttime periods. This is consistent with organic nitrates formed by NO_3 + BVOC (above) rapidly partitioning into the aerosol-phase.

BVOC measurements show large mixing ratios of isoprene throughout the entire campaign (daytime peaks above 8 ppb), followed by α- and β-pinene (peak nighttime mixing ratios of 0.5–1 ppb, Fig. S1). Using mixing ratios of VOC, which have well known reaction rates with NO_3, predicted NO_3 losses are calculated and compared to organic nitrate aerosol. Figure 4 shows the diurnally averaged NO_3 losses for the entire campaign period (1 June–15 July 2013). Daytime losses include photolysis and reaction with NO, however, approximately half the daytime losses are due to reaction of NO_3 with BVOC. Previous forest campaigns have assumed NO_3 + monoterpene reactions to be important only during the night and that isoprene, photolysis and NO losses were the only significant NO_3 sinks during the day (Geyer et al., 2001; Warneke et al., 2004), but in this study, we predict significant losses to BVOC during daylight hours.

To assess heterogeneous losses of N_2O_5 to particles, a kinetic uptake rate of N_2O_5 into deliquesced aerosols is estimated using PM surface area (S_A, $nm^2\,cm^{-3}$), the molecular speed of N_2O_5 ($\bar{c}$, $m\,s^{-1}$) and the uptake coefficient ($\gamma_{N_2O_5}$).

$$k_{het} = \frac{1}{4} \times \gamma_{N_2O_5} \times \bar{c}_{N_2O_5} \times S_A \qquad (5)$$

We used a value of $\gamma = 0.02$ as the uptake coefficient (Bertram and Thornton, 2009; Crowley et al., 2011) and represents an upper limit from previous field studies (Brown et al., 2009, 2006). We predict heterogeneous N_2O_5 uptake to be very small over the campaign despite high relative humidity. The highest uptake rates were calculated at $1.6 \times 10^{-3}\,s^{-1}$ in mid July, when $PM_{2.5}$ concentration was at its highest, and nevertheless represent less than 1 % of the losses of NO_3.

3.1.1 Calculation of NO_3 loss to BVOC

Using literature $NO_3 + BVOC$ rate coefficients and calculated $NO_{3,SS}$, we can calculate instantaneous NO_3 loss rates (($NO_{3,loss}$)$_{inst}$) for the campaign (Eq. 6). BVOC mixing ratios from GC-MS and rate constants shown in Table 1 were used to calculate the time-integrated nitrate loss to reactions with BVOC (Eq. 7). Specifically, time loss of NO_3 radical to reaction with BVOC (($NO_{3,loss}$)$_{integ}$, defined below in Eq. (7) were calculated during periods of increasing $RONO_2$ aerosol mass as monitored by AMS during SOAS. This buildup of aerosol $RONO_2$ was only observed after sunset. The boundary layer during night hours is relatively stable, such that NO_x and BVOC measurements can be considered an area-wide average and this simple box model can be used to calculate ($NO_{3,loss}$)$_{integ}$ (Eqs. 6 and 7). Under the assumption of a constant nighttime boundary layer height and an approximately uniform, area wide source that limits the time rate of change due to horizontal advection (i.e., a nighttime box), the time integrals of $RONO_2$ produced provide estimates of the evolution of $RONO_2$ concentrations at night. Times

of aerosol buildup were used determine time intervals for calculation of $(NO_{3,loss})_{integ}$.

$$(NO_{3,loss})_{inst} = \sum_i k_{NO_3+VOC_i}[VOC]_i[NO_3]_{SS} \qquad (6)$$

$$(NO_{3,loss})_{integ} = \sum_{i,t} (NO_{3,loss})_{inst,i} \times \Delta t \qquad (7)$$

$(NO_{3,loss})_{integ}$ is the calculated time integral of the reaction products of NO_3 with in-
dividual or combined mixing ratios of BVOC and Δt is the time step between each
calculated value of $(NO_{3,loss})_{inst,i}$. Data are averaged to 10 min increments, a time step
sufficient to resolve the observed rate of change. Figure 5 shows an example of the
resulting calculated integrated NO_3 losses from Eq. (7) to both isoprene and summed
monoterpenes, which are correlated with organic nitrate aerosol increases obtained
from AMS measurements. Note that these peak times occur during nighttime hours
when the boundary layer is shallow (Fig. S4).

Nightly total observed aerosol-phase organic nitrate buildups (Fig. 6) are plotted
against the predicted loss of NO_3 to monoterpenes. Linear fits and correlation coeffi-
cients aid in the interpretation of gas phase and aerosol phase organic nitrate forma-
tion. These correlations were made with $(NO_{3,loss})_{integ}$ to both isoprene and summed
monoterpenes (α-pinene, β-pinene, limonene and camphene).

The R^2 values in the individual species correlation plots suggest that first generation
monoterpene-derived organic nitrate products occur dominantly in the aerosol phase
over the gas phase (Fig. 7). This may be due to rapid partitioning of these species
to the aerosol phase, or to other rapid loss processes of these molecules in the gas
phase. The correlation plots in Fig. 6 are in ppb units, resulting in slopes that indicate
the average molar organic nitrate aerosol yield from monoterpenes. Using AMS and
TD-LIF measurements of aerosol phase organic nitrates gives a molar yield of 23 and
44 % respectively (Fig. 6) using all available data from each instrument. We note that
without knowledge of the average molecular weight of the aerosol organic nitrate, only
molar yield estimates are possible. We calculated our results using only monoterpenes,

Organic nitrate aerosol formation in the southeastern US

B. R. Ayres et al.

Title Page

Abstract | Introduction

Conclusions | References

Tables | Figures

|◄ | ►|

◄ | ►

Back | Close

Full Screen / Esc

Printer-friendly Version

Interactive Discussion

but the aerosols also contain sesquiterpene oxidation products and higher molecular weight BVOC products so SOA mass yields are likely to be higher. This comes about due to the condensing terpene oxidation products being more massive than the terpene precursors, and from multiple functional groups being needed to reduce the vapor pressure enough for substantial partitioning to the aerosol (Fry et al., 2013). Since nitrate product buildup occurs over multiple hours (Fig. 5), the rapid particulate organic nitrate losses (timescale of 2–4 h) found by Lee et al. (Lee et al., 2015) suggest that these molar yields are a lower limit. Furthermore, because this yield is based on total ambient monoterpene concentrations, it incorporates nitrate radical loss to α-pinene, which is known to produce very modest yields of SOA (0–10 %) from NO_3 reaction (Fry et al., 2014; Spittler et al., 2006). This suggests effective overall SOA yields from β-pinene, limonene and camphene are higher than 23–44 %.

3.1.2 Organic nitrate product analysis

Observations of $NO_{3,SS}$ compared to TD-LIF (Fig. 2) suggest aerosol organic nitrates are dominated by nighttime $NO_3 + BVOC$, rather than other known nitrate-producing reactions (e.g. $RO_2 + NO$), which would dominate during the daytime.

Specific first generation monoterpene organic nitrate compounds have been identified and measured in the gas and aerosol phases by CIMS (Lopez-Hilfiker et al., 2014; Lee et al., 2015). Using the $(NO_{3,loss})_{integ}$ calculations, a similar correlation analysis is conducted to identify key aerosol-producing products. Gas- and aerosol-phase organic nitrate concentrations from the CIMS are correlated with $(NO_{3,loss})_{integ}$ to monoterpenes (Fig. 7). The particle phase organic nitrates correlate better with the predicted monoterpene-nitrate production than gas phase (R^2 = 0.67 for particle phase $C_{10}H_{17}NO_5$ vs. 0.44 for gas phase). This is further evidence that uptake of monoterpene-nitrate compounds by aerosol takes place quickly after formation.

Less than 0.5 % of total particle-phase organic nitrates observed with the CIMS (Lee et al., 2015) were isoprene oxidation products, suggesting that most of the isoprene nitrate products remain in the gas phase. The correlation of gas-phase isoprene ni-

trate concentrations with NO_3 loss reveals the oxidative sources of these molecules (Fig. 8). The $C_5H_9NO_4$ isoprene product shows poor correlation with $(NO_{3,loss})_{integ}$ for isoprene ($R^2 = 0.02$), suggesting this is not a NO_3 radical product. However, $C_5H_9NO_5$ shows a good correlation with $(NO_{3,loss})_{integ}$ for isoprene ($R^2 = 0.70$) suggesting that this compound is a NO_3 oxidized product.

3.2 Comparison to inorganic NO_x sink: NO_3^- aerosol production from heterogeneous uptake of HNO_3

Partitioning of semivolatile ammonium nitrate into aerosol represented a small fraction of aerosol contribution throughout the campaign based on AMS data. A more important route of NO_x conversion to nitrate aerosol occurred via HNO_3 heterogeneous reaction on the surface of dust or sea salt particles (Scheme 1). This process, which was observed to be especially important during periods of high mineral or sea salt supermicron aerosol concentrations, is described in detail in a companion paper (Allen et al., 2015). Briefly, we observe that while concentrations of organic and inorganic nitrate aerosol are generally comparable (Figs. S2 and 3), the inorganic nitrate is more episodic in nature. Periods of highest NO_3^- concentration as measured by the MARGA were observed during two multi-day coarse-mode dust events, from 9 to 15 June and 23 to 30 June, while organic nitrates have a more regular diurnal pattern indicative of production from locally-available reactants, with most of the organic nitrate present in the condensed phase (data for gas- and aerosol-phase organic nitrate diurnally averaged for period of 1 to 15 July).

In order to estimate the fluxes of NO_x loss to aerosol via the two pathways shown in Scheme 1, we calculate the reactive losses of NO_2 to organic nitrate (limiting rate is taken to be $\sum_i k_i[NO_3][BVOC]_i$, with the included terpenes α-pinene, β-pinene, limonene and camphene) and to inorganic nitrate via heterogeneous HNO_3 uptake (Allen et al., 2015). A substantial fraction of the suface area is in the transition regime, so HNO_3 uptake is reduced due to diffusion limitations. To account for this, a Fuchs–

Sutugin correction is applied (Seinfeld and Pandis, 2006):

$$\text{Rate} = \sum^{R_p} \frac{S_a}{R_p} D_g \left(\frac{0.75\alpha \, (1 + \text{Kn})}{\text{Kn}^2 + \text{Kn} + 0.283\text{Kn} \, \alpha + 0.75\alpha} \right) [\text{HNO}_3] \quad \text{(R2)}$$

with S_a is surface area, R_p is the radius, D_g is the diffusivity of HNO_3 in air ($0.118\,\text{cm}^2\,\text{s}^{-1}$) and α is estimated at 0.1 for an upper limit.

Since we have seen that the organic nitrates are present predominantly in the condensed phase, we take this comparison to be the relative rate of production of organic nitrate aerosol vs. inorganic nitrate aerosol (Fig. 9), and we see that over the summer campaign, the rates are comparable in magnitude, but peak at different times. This analysis suggests that substantial nitrate aerosol (peak values of $1\,\mu\text{g m}^{-3}\text{hr}^{-1}$, with average rates $0.1\,\mu\text{g m}^{-3}\text{hr}^{-1}$ for both inorganic and organic nitrate rates) is produced in the southeastern US by both inorganic and organic routes (depicted in Scheme 1), converting local NO_x pollution to particulate matter. We note that this calculation accounts only for the production rates of these two types of nitrate aerosol and does not account for subsequent chemistry that may deplete one faster than the other; hence, relative mass concentrations are not necessarily expected to correlate directly to these relative production rates.

3.3 Implications of NO_3 oxidation on SOA formation in the southeastern US

The $NO_3 + BVOC$ reaction in the troposphere has become increasingly noted as a source of SOA in recent years (Beaver et al., 2012; Fry et al., 2013; Rollins et al., 2012). In 2010, Pye et al. showed current models which include NO_3 radical oxidation increase predicted SOA yields from terpenes by 100 % and total aerosol concentrations by 30 % (Pye et al., 2010). The results of our study help to underscore the importance of NO_3 in SOA formation. As discussed above, measured aerosol organonitrate concentrations show that NO_3 oxidation produces substantial SOA (23–44 % molar yield).

This pathway is especially important before sunrise when competing oxidants (O_3 and OH) are at a minimum.

We calculate a rough estimate of the contribution of NO_x to PM via this NO_3 + BVOC mechanism based on 2011 NEI data for the states included in the 2004 Southern Appalachian Mountain Initiative study (SAMI, Odman et al., 2004): Kentucky, Virginia, West Virginia, North Carolina, South Carolina, Tennessee, Alabama and Georgia (http://www.epa.gov/ttn/chief/net/2011inventory.html). This comparator study was chosen because it is the region that includes the SOAS field site. In this 8-state region, the NEI reported $2.3\,\mathrm{Tg\,yr^{-1}}$ ($2.5 \times 10^6\,\mathrm{tons\,yr^{-1}}$) of nitrogen oxides in 2011 from Criteria based emissions of pollutants. The EPA also reported $0.8\,\mathrm{Tg\,yr^{-1}}$ ($9 \times 10^5\,\mathrm{tons\,yr^{-1}}$) of $PM_{2.5}$. We estimate the fraction of NO_x converted to PM using several assumptions. NO_2 is estimated to contribute 50 % of the NO_y budget (Fig. S2), so we multiply the NO_x emission by 0.5 to account for half of the instantaneous NO_x residing in the atmosphere as other NO_y species at any given time. An average lifetime of 16 h for $O_3 + NO_2$ reaction was calculated ($1/k[O_3]$) and, with an average nighttime length of 9 h, we estimate about 55 % of NO_2 is converted to NO_3 overnight. Using the average molar organic nitrate aerosol yield of 30 % determined in this study and an estimated molecular weight of $250\,\mathrm{g\,mol^{-1}}$ for oxidized product (terpene hydoxynitrate with two additional oxygen functional groups, Draper et al., 2015), we convert from molar yield to mass yield of organic nitrate aerosol. Finally, using the summed NEI NO_x emissions data for the SAMI states, we calculate a source estimate of $0.6\,\mathrm{Tg\,yr^{-1}}$ of NO_3-oxidized aerosol. Adding this to the NEI primary $PM_{2.5}$ emissions estimate of $0.8\,\mathrm{Tg\,yr^{-1}}$ gives a total $1.4\,\mathrm{Tg\,yr^{-1}}$, showing that NO_3 initiated SOA formation would contribute a substantial additional source of $PM_{2.5}$ regionally, nearly doubling primary emissions. Model calculations by Odman et al. (2004) for the SAMI states estimated $1\,\mathrm{Tg\,yr^{-1}}$ of total $PM_{2.5}$ in 2010, including primary and secondary sources. Their modeled $PM_{2.5}$ emissions are lower than our rough estimate here, despite the fact that actual 2010 NO_x emissions were $2.3\,\mathrm{Tg\,yr^{-1}}$ rather than the $3\,\mathrm{Tg\,yr^{-1}}$ projected at that time. Hence, despite successful reduction of regional NO_x emissions (Blanchard et al., 2013), this work

suggests that secondary $PM_{2.5}$ production from NO_3 oxidation of regionally abundant BVOCs remains a substantial anthropogenic source of pollution in the southeastern US.

4 Conclusions

5 The contribution of NO_3 + BVOC to SOA formation is found to be substantial in the terpene-rich southeastern US. An estimated 23–44 % of nitrate radical lost to reaction with monoterpenes becomes aerosol-phase organic nitrate. A predicted nitrate loss to terpenes is calculated from the steady-state nitrate and terpene mixing ratios and then time integrated during evenings and nights as $RONO_2$ aerosol builds up. Nitrate losses
10 are correlated to CIMS, TD-LIF and AMS measurements of gas- and aerosol-phase organic nitrate and show good agreement between $(NO_{3,loss})_{integ}$ to monoterpene and total aerosol organic nitrate maxima. The main structure found in the aerosol phase, as measured by CIMS, is $C_{10}H_{17}NO_5$, which correlates well with cumulative $(NO_{3,loss})_{integ}$. This NO_3 + BVOC source of nitrate aerosol is comparable in magnitude to inorganic
15 nitrate aerosol formation, and is observed to be a substantial contribution to regional $PM_{2.5}$.

The Supplement related to this article is available online at doi:10.5194/acpd-15-16235-2015-supplement.

References

Ahmadov, R., McKeen, S. A., Robinson, A. L., Bahreini, R., Middlebrook, A. M., de Gouw, J. A., Meagher, J., Hsie, E.-Y., Edgerton, E., Shaw, S., and Trainer, M.: A volatility basis set model for summertime secondary organic aerosols over the eastern United States in 2006, J. Geophys. Res., 117, D06301, doi:10.1029/2011JD016831, 2012. 16238

Aldener, M., Brown, S. S., Stark, H., Williams, E., Lerner, B., Kuster, W., Goldan, P., Quinn, P., Bates, T., and Fehsenfeld, F.: Reactivity and loss mechanisms of NO_3 and N_2O_5 in a polluted marine environment: results from in situ measurements during New England Air Quality Study 2002, J. Geophys. Res.-Atmos., 111, D23S73, doi:10.1029/2006JD007252, 2006. 16239

Allen, H. M., Draper, D. C., Ayres, B., Takehama, S., Mondini, R., Ergin, G., Baumann, K., Edgerson, E., Knote, C., Ault, A., Bond, A., and Fry, J. L.: Influence of aerosol acidity and mineral or sea-salt supermicron particle concentrations on inorganic NO_3 aerosol during the 2013 Southern Oxidant and Aerosol Study, Atmos. Chem. Phys. Discuss., 15, 13827–13865, doi:10.5194/acpd-15-13827-2015, 2015. 16240, 16248

Atkinson, R. and Arey, J.: Atmospheric chemistry of biogenic organic compounds, Accounts Chem. Res., 31, 574–583, 1998. 16238

Atkinson, R. and Arey, J.: Gas-phase tropospheric chemistry of biogenic volatile organic compounds: a review, Atmos. Environ., 37, 197–219, 2003. 16238

Bahreini, R., Dunlea, E. J., Matthew, B. M., Simons, C., Docherty, K., DeCarlo, P. F., Jimenez, J. L., Brock, C. A., and M.Middlebrook, A.: Design and operation of a pressure-controlled inlet for airborne sampling with an aerodynamic aerosol lens, Aerosol Sci. Tech., 42, 465–471, 2008. 16239

Beaver, M. R., Clair, J. M. St., Paulot, F., Spencer, K. M., Crounse, J. D., LaFranchi, B. W., Min, K. E., Pusede, S. E., Wooldridge, P. J., Schade, G. W., Park, C., Cohen, R. C., and Wennberg, P. O.: Importance of biogenic precursors to the budget of organic nitrates: observations of multifunctional organic nitrates by CIMS and TD-LIF during BEARPEX 2009, Atmos. Chem. Phys., 12, 5773–5785, doi:10.5194/acp-12-5773-2012, 2012. 16239, 16241, 16249

Bellouin, N., Rae, J., Jones, A., Johnson, C., Haywood, J., and Boucher, O.: Aerosol forcing in the Climate Model Intercomparison Project (CMIP5) simulations by HadGEM2-ES and

the role of ammonium nitrate, J. Geophys. Res., 116, D20206, doi:10.1029/2011JD016074, 2011. 16237

Bertram, T. H. and Thornton, J. A.: Toward a general parameterization of N_2O_5 reactivity on aqueous particles: the competing effects of particle liquid water, nitrate and chloride, Atmos. Chem. Phys., 9, 8351–8363, doi:10.5194/acp-9-8351-2009, 2009. 16245

Bertram, T. H., Kimmel, J. R., Crisp, T. A., Ryder, O. S., Yatavelli, R. L. N., Thornton, J. A., Cubison, M. J., Gonin, M., and Worsnop, D. R.: A field-deployable, chemical ionization time-of-flight mass spectrometer, Atmos. Meas. Tech., 4, 1471–1479, doi:10.5194/amt-4-1471-2011, 2011. 16241

Blanchard, C., Hidy, G., Tanenbaum, S., Edgerton, E., and Hartsell, B.: The Southeastern Aerosol Research and Characterization (SEARCH) study: temporal trends in gas and PM concentrations and composition, 1999–2010, JAPCA J. Air Waste Ma., 63, 247–259, 2013. 16239, 16250

Boyd, C. M., Sanchez, J., Xu, L., Eugene, A. J., Nah, T., Tuet, W. Y., Guzman, M. I., and Ng, N. L.: Secondary Organic Aerosol (SOA) formation from the β-pinene + NO_3 system: effect of humidity and peroxy radical fate, Atmos. Chem. Phys. Discuss., 15, 2679–2744, doi:10.5194/acpd-15-2679-2015, 2015. 16238

Brown, S. S. and Stutz, J.: Nighttime radical observations and chemistry, Chem. Soc. Rev., 41, 6405–6447, 2012. 16239

Brown, S. S., Osthoff, H. D., Stark, H., Dubé, W. P., Ryerson, T. B., Warneke, C., de Gouw, J. A., Wollny, A. G., Parrish, D. D., Fehsenfeld, F. C., and Ravishankara, A. R.: Aircraft observations of daytime NO_3 and N_2O_5 and their implications for tropospheric chemistry, J. Photochem. Photobio. A, 176, 270–278, 2005. 16239

Brown, S. S., Ryerson, T. B., Wollny, A. G., Brock, C. A., Peltier, R., Sullivan, A. P., Weber, R. J., Dubé, W. P., Trainer, M., Meagher, J. F., Fehsenfeld, F. C., and Ravishankara, A. R.: Variability in nocturnal nitrogen oxide processing and its role in regional air quality, Science, 311, 67–70, 2006. 16245

Brown, S. S., Dubé, W., Fuchs, H., Ryerson, T., Wollny, A., Brock, C., Bahreini, R., Middlebrook, A., Neuman, J., and Atlas, E.: Reactive uptake coefficients for N_2O_5 determined from aircraft measurements during the Second Texas Air Quality Study: comparison to current model parameterizations, J. Geophys. Res.-Atmos., 114, D00F10, doi:10.1029/2008JD011679, 2009. 16245

Calogirou, A., Larsen, B. R., and Kotzias, D.: Gas-phase terpene oxidation products: a review, Atmos. Environ., 33, 1423–1439, 1999. 16238

Calvert, J. G., Atkinson, R., Kerr, J. A., Madronich, S., Moortgat, G. K., Wallington, T. J., and Yarwood, G.: The Mechanisms of Atmospheric Oxidation of the Alkenes, Oxford University Press, New York, 2000. 16262

Carlton, A. G., Pinder, R. W., Bhave, P. V., and Pouliot, G. A.: To what extent can biogenic SOA be controlled?, Environ. Sci. Technol., 44, 3376–3380, 2010. 16238

Chameides, W. L.: Photo-chemical role of tropospheric nitrogen-oxides, Geophys. Res. Lett., 5, 17–20, 1978. 16238

Crounse, J. D., McKinney, K. A., Kwan, A. J., and Wennberg, P. O.: Measurement of gas-phase hydroperoxides by chemical ionization mass spectrometry, Anal. Chem., 78, 6726–6732, 2006. 16241

Crounse, J. D., Nielsen, L. B., and Jørgensen, S.: Autoxidation of organic compounds in the atmosphere, J. Phys. Chem. Lett., 4, 3513–3520, 2013. 16241

Crowley, J. N., Thieser, J., Tang, M. J., Schuster, G., Bozem, H., Beygi, Z. H., Fischer, H., Diesch, J.-M., Drewnick, F., Borrmann, S., Song, W., Yassaa, N., Williams, J., Pöhler, D., Platt, U., and Lelieveld, J.: Variable lifetimes and loss mechanisms for NO_3 and N_2O_5 during the DOMINO campaign: contrasts between marine, urban and continental air, Atmos. Chem. Phys., 11, 10853–10870, doi:10.5194/acp-11-10853-2011, 2011. 16245

Crutzen, P. J. and Andreae, M. O.: Biomass burning in the tropics – impact on atmospheric chemistry and biogeochemical cycles, Science, 250, 1669–1678, 1990. 16239

Dallmann, T., DeMartini, S., Kirchstetter, T., Herndon, S., Onasch, T., Wood, E., and Harley, R.: On-road measurement of gas and particle phase pollutant emission factors for individual heavy-duty diesel trucks, Environ. Sci. Technol., 46, 8511–8518, 2012. 16239

Das, M. and Aneja, V.: Regional analysis of nonmethane volatile organic compounds in the lower troposphere of the Southeast United States, J. Environ. Eng.-ASCE, 129, 1085–1103, 2003. 16240

Day, D. A., Wooldridge, P. J., Dillon, M. B., Thornton, J. A., and Cohen, R. C.: A thermal dissociation laser-induced fluorescence instrument for in situ detection of NO_2, peroxy nitrates, alkyl nitrates, and HNO_3, J. Geophys. Res.-Atmos., 107, ACH-4-1–ACH-4-14, doi:10.1029/2001JD000779, 2002. 16239, 16241

DeCarlo, P. F., Kimmel, J. R., Trimborn, A., Northway, M. J., Jayne, J. T., Aiken, A. C., Gonin, M., Fuhrer, K., Horvath, T., Docherty, K. S., Worsnop, D. R., and Jimenez, J. L.:

Title Page

Abstract | Introduction

Conclusions | References

Tables | Figures

|◀ | ▶|

◀ | ▶

Back | Close

Full Screen / Esc

Printer-friendly Version

Interactive Discussion

Field-deployable, high-resolution, time-of-flight aerosol mass spectrometer, Anal. Chem., 78, 8281–8289, 2006. 16241

De Gouw, J. A.: Budget of organic carbon in a polluted atmosphere: results from the New England Air Quality Study in 2002, J. Geophys. Res., 110, D16305, doi:10.1029/2004JD005623, 2005. 16238

Draper, D. C., Farmer, D. K., Desyaterik, Y., and Fry, J. L.: A comparison of secondary organic aerosol (SOA) yields and composition from ozonolysis of monoterpenes at varying concentrations of NO2, Atmos. Chem. Phys. Discuss., 15, 14923–14960, doi:10.5194/acpd-15-14923-2015, 2015. 16250

Eddingsaas, N. C., Loza, C. L., Yee, L. D., Seinfeld, J. H., and Wennberg, P. O.: α-pinene photooxidation under controlled chemical conditions – Part 1: Gas-phase composition in low- and high-NO$_x$ environments, Atmos. Chem. Phys., 12, 6489–6504, doi:10.5194/acp-12-6489-2012, 2012. 16241

Farmer, D., Matsunaga, A., Docherty, K., Surratt, J., Seinfeld, J., Ziemann, P., and Jimenez, J.: Response of an aerosol mass spectrometer to organonitrates and organosulfates and implications for atmospheric chemistry, P. Natl. Acad. Sci. USA, 107, 6670–6675, 2010. 16239, 16241

Feng, Y. and Penner, J. E.: Global modeling of nitrate and ammonium: interaction of aerosols and tropospheric chemistry, J. Geophys. Res.-Atmos., 112, D01304, doi:10.1029/2005JD006404, 2007. 16237

Fry, J. L., Kiendler-Scharr, A., Rollins, A. W., Wooldridge, P. J., Brown, S. S., Fuchs, H., Dubé, W., Mensah, A., dal Maso, M., Tillmann, R., Dorn, H.-P., Brauers, T., and Cohen, R. C.: Organic nitrate and secondary organic aerosol yield from NO$_3$ oxidation of β-pinene evaluated using a gas-phase kinetics/aerosol partitioning model, Atmos. Chem. Phys., 9, 1431–1449, doi:10.5194/acp-9-1431-2009, 2009. 16238

Fry, J. L., Kiendler-Scharr, A., Rollins, A. W., Brauers, T., Brown, S. S., Dorn, H.-P., Dubé, W. P., Fuchs, H., Mensah, A., Rohrer, F., Tillmann, R., Wahner, A., Wooldridge, P. J., and Cohen, R. C.: SOA from limonene: role of NO$_3$ in its generation and degradation, Atmos. Chem. Phys., 11, 3879–3894, doi:10.5194/acp-11-3879-2011, 2011. 16238

Fry, J. L., Draper, D. C., Zarzana, K. J., Campuzano-Jost, P., Day, D. A., Jimenez, J. L., Brown, S. S., Cohen, R. C., Kaser, L., Hansel, A., Cappellin, L., Karl, T., Hodzic Roux, A., Turnipseed, A., Cantrell, C., Lefer, B. L., and Grossberg, N.: Observations of gas- and aerosol-phase or-

Title Page

Abstract | Introduction

Conclusions | References

Tables | Figures

|◄ | ►|

◄ | ►

Back | Close

Full Screen / Esc

Printer-friendly Version

Interactive Discussion

ganic nitrates at BEACHON-RoMBAS 2011, Atmos. Chem. Phys. Discuss., 13, 1979–2034, doi:10.5194/acpd-13-1979-2013, 2013. 16241, 16247, 16249

Fry, J. L., Draper, D. C., Barsanti, K. C., Smith, J. N., Ortega, J., Winkler, P. M., Lawler, M. J., Brown, S. S., Edwards, P. M., Cohen, R. C., and Lee, L.: Secondary organic aerosol formation and organic nitrate yield from NO_3 oxidation of biogenic hydrocarbons, Environ. Sci. Technol., 48, 11944–11953, 2014. 16247

Geyer, A., Alicke, B., Konrad, S., Schmitz, T., Stutz, J., and Platt, U.: Chemistry and oxidation capacity of the nitrate radical in the continental boundary layer near Berlin, J. Geophys. Res.-Atmos., 106, 8013–8025, 2001. 16244

Gilman, J. B., Burkhart, J. F., Lerner, B. M., Williams, E. J., Kuster, W. C., Goldan, P. D., Murphy, P. C., Warneke, C., Fowler, C., Montzka, S. A., Miller, B. R., Miller, L., Oltmans, S. J., Ryerson, T. B., Cooper, O. R., Stohl, A., and de Gouw, J. A.: Ozone variability and halogen oxidation within the Arctic and sub-Arctic springtime boundary layer, Atmos. Chem. Phys., 10, 10223–10236, doi:10.5194/acp-10-10223-2010, 2010. 16241

Goldan, P. D., Kuster, W. C., Fehsenfeld, F. C., and Montzka, S. A.: Hydrocarbon measurements in the southeastern United States: the Rural Oxidants in the Southern Environment (ROSE) Program 1990, J. Geophys. Res.-Atmos., 100, 25945, doi:10.1029/95JD02607, 1995. 16241

Goldan, P. D., Kuster, W. C., Williams, E., Murphy, P. C., Fehsenfeld, F. C., and Meagher, J.: Nonmethane hydrocarbon and oxy hydrocarbon measurements during the 2002 New England Air Quality Study, J. Geophys. Res.-Atmos., 109, D21309, doi:10.1029/2003JD004455, 2004. 16241

Goldstein, A. H. and Galbally, I. E.: Known and unexplored organic constituents in the earth's atmosphere, Environ. Sci. Technol., 41, 1514–1521, 2007. 16238

Goldstein, A. H., Koven, C., Heald, C., and Fung, I.: Biogenic carbon and anthropogenic pollutants combine to form a cooling haze over the southeastern United States, P. Natl. Acad. Sci. USA, 106, 8835–8840, 2009. 16237

Griffin, R. J., Cocker III, D. R., Flagan, R. C., and Seinfeld, J. H.: Organic aerosol formation from the oxidation of biogenic hydrocarbons, J. Geophys. Res.-Atmos., 104, 3555–3567, 1999. 16238

Hallquist, M., Wenger, J. C., Baltensperger, U., Rudich, Y., Simpson, D., Claeys, M., Dommen, J., Donahue, N. M., George, C., Goldstein, A. H., Hamilton, J. F., Herrmann, H., Hoffmann, T., Iinuma, Y., Jang, M., Jenkin, M. E., Jimenez, J. L., Kiendler-Scharr, A., Maenhaut, W., McFiggans, G., Mentel, Th. F., Monod, A., Prévôt, A. S. H., Seinfeld, J. H., Sur-

ratt, J. D., Szmigielski, R., and Wildt, J.: The formation, properties and impact of secondary organic aerosol: current and emerging issues, Atmos. Chem. Phys., 9, 5155–5236, doi:10.5194/acp-9-5155-2009, 2009. 16238

Heald, C. L., Jacob, D. J., Park, R. J., Russell, L. M., Huebert, B. J., Seinfeld, J. H., Liao, H., and Weber, R. J.: A large organic aerosol source in the free troposphere missing from current models, Geophys. Res. Lett., 32, L18809, doi:10.1029/2005GL023831, 2005. 16238

Hidy, G. M., Blanchard, C. L., Baumann, K., Edgerton, E., Tanenbaum, S., Shaw, S., Knipping, E., Tombach, I., Jansen, J., and Walters, J.: Chemical climatology of the southeastern United States, 1999–2013, Atmos. Chem. Phys., 14, 11893–11914, doi:10.5194/acp-14-11893-2014, 2014. 16240

Jimenez, J. L., Canagaratna, M. R., Donahue, N. M., Prevot, A. S. H., Zhang, Q., Kroll, J. H., DeCarlo, P. F., Allan, J. D., Coe, H., Ng, N. L., Aiken, A. C., Docherty, K. S., Ulbrich, I. M., Grieshop, A. P., Robinson, A. L., Duplissy, J., Smith, J. D., Wilson, K. R., Lanz, V. A., Hueglin, C., Sun, Y. L., Tian, J., Laaksonen, A., Raatikainen, T., Rautiainen, J., Vaattovaara, P., Ehn, M., Kulmala, M., Tomlinson, J. M., Collins, D. R., Cubison, M. J., Dunlea, E. J., Huffman, J. A., Onasch, T. B., Alfarra, M. R., Williams, P. I., Bower, K., Kondo, Y., Schneider, J., Drewnick, F., Borrmann, S., Weimer, S., Demerjian, K., Salcedo, D., Cottrell, L., Griffin, R., Takami, A., Miyoshi, T., Hatakeyama, S., Shimono, A., Sun, J. Y., Zhang, Y. M., Dzepina, K., Kimmel, J. R., Sueper, D., Jayne, J. T., Herndon, S. C., Trimborn, A. M., Williams, L. R., Wood, E. C., Middlebrook, A. M., Kolb, C. E., Baltensperger, U., and Worsnop, D. R.: Evolution of organic aerosols in the atmosphere, Science, 326, 1525–1529, 2009. 16238

Kroll, J. H. and Seinfeld, J. H.: Chemistry of secondary organic aerosol: formation and evolution of low-volatility organics in the atmosphere, Atmos. Environ., 42, 3593–3624, 2008. 16239

Lee, B. H., Mohr, C., Lopez-Hilfiker, F. D., Lutz, A., Hallquist, M., Hu, W. W., Jimenez, J., Xu, L., Ng, N. L., Romer, P., Cohen, R. C., Wild, R. J., Kim, S., de Gouw, J., Goldstein, A. H., Shepson, P. B., Wennberg, P. O., and Thornton, J. A.: Highly functionalized particle-phase organic nitrates observed in the Southeastern US: contribution to secondary organic aerosol and reactive nitrogen budgets, in preparation, 2015. 16239, 16247

Lee, T., Yu, X.-Y., Ayres, B., Kreidenweis, S., Malm, W., and Collett Jr., J.: Observations of fine and coarse particle nitrate at several rural locations in the United States, Atmos. Environ., 42, 2720–2732, 2008. 16238

Organic nitrate aerosol formation in the southeastern US

B. R. Ayres et al.

Title Page

Abstract	Introduction
Conclusions	References
Tables	Figures

|◄ ►|

◄ ►

Back Close

Full Screen / Esc

Printer-friendly Version

Interactive Discussion

Lopez-Hilfiker, F. D., Mohr, C., Ehn, M., Rubach, F., Kleist, E., Wildt, J., Mentel, Th. F., Lutz, A., Hallquist, M., Worsnop, D., and Thornton, J. A.: A novel method for online analysis of gas and particle composition: description and evaluation of a Filter Inlet for Gases and AEROsols (FIGAERO), Atmos. Meas. Tech., 7, 983–1001, doi:10.5194/amt-7-983-2014, 2014. 16241, 16247

Makkonen, U., Virkkula, A., Mäntykenttä, J., Hakola, H., Keronen, P., Vakkari, V., and Aalto, P. P.: Semi-continuous gas and inorganic aerosol measurements at a Finnish urban site: comparisons with filters, nitrogen in aerosol and gas phases, and aerosol acidity, Atmos. Chem. Phys., 12, 5617–5631, doi:10.5194/acp-12-5617-2012, 2012. 16239, 16242

Myhre, G., Samset, B. H., Schulz, M., Balkanski, Y., Bauer, S., Berntsen, T. K., Bian, H., Bellouin, N., Chin, M., Diehl, T., Easter, R. C., Feichter, J., Ghan, S. J., Hauglustaine, D., Iversen, T., Kinne, S., Kirkevåg, A., Lamarque, J.-F., Lin, G., Liu, X., Lund, M. T., Luo, G., Ma, X., van Noije, T., Penner, J. E., Rasch, P. J., Ruiz, A., Seland, Ø., Skeie, R. B., Stier, P., Takemura, T., Tsigaridis, K., Wang, P., Wang, Z., Xu, L., Yu, H., Yu, F., Yoon, J.-H., Zhang, K., Zhang, H., and Zhou, C.: Radiative forcing of the direct aerosol effect from AeroCom Phase II simulations, Atmos. Chem. Phys., 13, 1853–1877, doi:10.5194/acp-13-1853-2013, 2013. 16237

Nel, A.: Atmosphere. air pollution-related illness: effects of particles, Science, 308, 804–806, 2005. 16237

Odman, M. T., Boylan, J. W., and Russell, A. G.: Air Pollution Modeling and Its Application XVI, Springer, New York, USA, 16 edn., 2004. 16250

Perring, A. E., Pusede, S. E., and Cohen, R. C.: An observational perspective on the atmospheric impacts of alkyl and multifunctional nitrates on ozone and secondary organic aerosol, Chem. Rev., 113, 5848–5870, 2013. 16239

Pope, C. A. and Dockery, D. W.: Health effects of fine particulate air pollution: lines that connect, JAPCA J. Air Waste Ma., 56, 709–742, 2006. 16238

Pye, H. O. T., Chan, A. W. H., Barkley, M. P., and Seinfeld, J. H.: Global modeling of organic aerosol: the importance of reactive nitrogen (NO_x and NO_3), Atmos. Chem. Phys., 10, 11261–11276, doi:10.5194/acp-10-11261-2010, 2010. 16249

Rollins, A. W., Smith, J. D., Wilson, K. R., and Cohen, R. C.: Real time in situ detection of organic nitrates in atmospheric aerosols, Environ. Sci. Technol., 44, 5540–5545, 2010. 16239, 16241

Rollins, A. W., Browne, E. C., Min, K.-E., Pusede, S. E., Wooldridge, P. J., Gentner, D. R., Goldstein, A. H., Liu, S., Day, D. A., Russell, L. M., and Cohen, R. C.: Evidence for NO_x

Control over Nighttime SOA Formation, Science, 337, 1210, doi:10.1126/science.1221520, 2012. 16238, 16241, 16249

Sander, S. P., Friedl, R. R., Barker, J. R., Golden, D. M., Kurylo, M. J., Wine, P. H., Abbatt, J. P. D., Burkholder, J. B., Kolb, C. E., Moortgat, G. K., Huie, R. E., and Orkin, V. L.: Chemical Kinetics and Photochemical Data for Use in Atmospheric Studies – Evaluation Number 17, JPL Publication 10-6, Pasadena, California, USA, 1–684, 2011. 16244, 16262

Saunders, S. M., Jenkin, M. E., Derwent, R. G., and Pilling, M. J.: Protocol for the development of the Master Chemical Mechanism, MCM v3 (Part A): tropospheric degradation of non-aromatic volatile organic compounds, Atmos. Chem. Phys., 3, 161–180, doi:10.5194/acp-3-161-2003, 2003. 16243

Seinfeld, J. H. and Pandis, S. N.: Atmospheric Chemistry and Physics: From Air Pollution to Climate Change, John Wiley and Sons, Inc., Hoboken, New Jersey, USA, 2nd edn., 2006. 16249

Spittler, M., Barnes, I., Bejan, I., Brockmann, K., Benter, T., and Wirtz, K.: Reactions of NO_3 radicals with limonene and α-pinene: product and SOA formation, Atmos. Environ., 40, S116–S127, 2006. 16247

Spracklen, D. V., Jimenez, J. L., Carslaw, K. S., Worsnop, D. R., Evans, M. J., Mann, G. W., Zhang, Q., Canagaratna, M. R., Allan, J., Coe, H., McFiggans, G., Rap, A., and Forster, P.: Aerosol mass spectrometer constraint on the global secondary organic aerosol budget, Atmos. Chem. Phys., 11, 12109–12136, doi:10.5194/acp-11-12109-2011, 2011. 16238

Stanier, C. O., Khlystov, A. Y., Chan, W. R., Mandiro, M., and Pandis, S. N.: A method for the in situ measurement of fine aerosol water content of ambient aerosols: The dry-ambient aerosol size spectrometer (DAASS), Aerosol Sci. Tech., 38, 215–228, 2004. 16242

Stocker, T. F., Qin, D., Plattner, G.-K., Tignor, M. M. B., Allen, S. K., Boschung, J., Nauels, A., Xia, Y., Bex, V., and Midgley, P. M. (Eds.): Climate Change 2013: The Physical Science Basis, Working Group I Contribution to the Fifth Assessment Report of the Intergovernmental Panel on Climate Change, Cambridge University Press, Cambridge, UK, 2013. 16238

Stroud, C., Roberts, J., Williams, E., Hereid, D., Angevine, W., Fehsenfeld, F., Wisthaler, A. A., Hansel, Martinez-Harder, M., Harder, H., Brune, W., Hoenninger, G., Stutz, J., and White, A.: Nighttime isoprene trends at an urban forested site during the 1999 Southern Oxidant Study, J. Geophys. Res.-Atmos., 107, D16, doi:10.1029/2001JD000959, 2002. 16241

Organic nitrate aerosol formation in the southeastern US

B. R. Ayres et al.

Title Page

Abstract	Introduction
Conclusions	References
Tables	Figures

Back | Close

Full Screen / Esc

Printer-friendly Version

Interactive Discussion

Trebs, I., Meixner, F. X., Slanina, J., Otjes, R., Jongejan, P., and Andreae, M. O.: Real-time measurements of ammonia, acidic trace gases and water-soluble inorganic aerosol species at a rural site in the Amazon Basin, Atmos. Chem. Phys., 4, 967–987, doi:10.5194/acp-4-967-2004, 2004. 16239, 16242

5 Vlasenko, A., Sjogren, S., Weingartner, E., Stemmler, K., Gäggeler, H. W., and Ammann, M.: Effect of humidity on nitric acid uptake to mineral dust aerosol particles, Atmos. Chem. Phys., 6, 2147–2160, doi:10.5194/acp-6-2147-2006, 2006. 16238

Wagner, N. L., Dubé, W. P., Washenfelder, R. A., Young, C. J., Pollack, I. B., Ryerson, T. B., and Brown, S. S.: Diode laser-based cavity ring-down instrument for NO_3, N_2O_5, NO, NO_2 and

10 O_3 from aircraft, Atmos. Meas. Tech., 4, 1227–1240, doi:10.5194/amt-4-1227-2011, 2011. 16241

Warneke, C., De Gouw, J. A., Goldan, P. D., Kuster, W. C., Williams, E. J., Lerner, B. M., Jakoubek, R., Brown, S. S., Stark, H., Aldener, M., Ravishankara, A. R., Roberts, J. M., Marchewka, M., Bertman, S., Sueper, D. T., McKeen, S. A., Meagher, J. F., and Fehsen-

15 feld, F. C.: Comparison of daytime and nighttime oxidation of biogenic and anthropogenic VOCs along the New England coast in summer during New England Air Quality Study 2002, J. Geophys. Res.-Atmos., 109, D10309, doi:10.1029/2003JD004424, 2004. 16244

Wild, R., Edwards, P., Dubé, W., Baumann, K., Edgerton, E., Quinn, P., Roberts, J., Rollins, A., Veres, P., Warneke, C., Williams, E., Yuan, B., and Brown, S.: A measurement of total reactive

20 nitrogen, NO_y, together with NO_2, NO and O_3 via cavity ring-down spectroscopy, Environ. Sci. Technol., 48, 9609–9615, 2014. 16241

Winer, A. M., Atkinson, R., James, N., and Pitts, J.: Gaseous nitrate radical: possible nighttime atmospheric sink for biogenic organic compounds, Science, 224, 156–159, 1984. 16238

Yatavelli, R., Lopez-Hilfiker, F., Wargo, J., Kimmel, J., Cubison, M., Bertram, T., Jimenez, J.,

25 Gonin, M., Worsnop, D., and Thornton, J.: A chemical ionization high-resolution time-of-flight mass spectrometer coupled to a Micro Orifice Volatilization Impactor (MOVI-HRToF-CIMS) for analysis of gas and particle-phase organic species, Aerosol Sci. Tech., 46, 1313–1327, 2012. 16241

Zhang, Q., Jimenez, J. L., Canagaratna, M. R., Allan, J. D., Coe, H., Ulbrich, I., Alfarra, M. R.,

30 Takami, A., Middlebrook, A. M., Sun, Y. L., Dzepina, K., Dunlea, E., Docherty, K., De-Carlo, P. F., Salcedo, D., Onasch, T., Jayne, J. T., Miyoshi, T., Shimono, A., Hatakeyama, S., Takegawa, N., Kondo, Y., Schneider, J., Drewnick, F., Borrmann, S., Weimer, S., Demer-jian, K., Williams, P., Bower, K., Bahreini, R., Cottrell, L., Griffin, R. J., Rautiainen, J.,

Organic nitrate aerosol formation in the southeastern US

B. R. Ayres et al.

Title Page

Abstract | Introduction

Conclusions | References

Tables | Figures

Back | Close

Full Screen / Esc

Printer-friendly Version

Interactive Discussion

Sun, J. Y., Zhang, Y. M., and Worsnop, D. R.: Ubiquity and dominance of oxygenated species in organic aerosols in anthropogenically-influenced Northern Hemisphere midlatitudes, Geophys. Res. Lett., 34, L13801, doi:10.1029/2007GL029979, 2007. 16238

Table 1. NO_3 kinetic rate constants and equilibrium constants used to determine losses.

Reaction	A	E/R [a]	B [b]	$k(298\,\text{K})$	Source
$O_3 + NO_2 \rightarrow O_2 + NO_3$	1.2×10^{-13}	2450			Sander et al. (2011)
$NO_3 + NO_2 \rightleftharpoons N_2O_5$	2.7×10^{-27}		11 000		Sander et al. (2011)
$NO + NO_3 \rightarrow 2NO_2$	1.5×10^{-11}	−170			Sander et al. (2011)
Isoprene + $NO_3 \rightarrow$ Products	3.03×10^{-12}	446			Calvert et al. (2000)
α-pinene + $NO_3 \rightarrow$ Products	1.19×10^{-12}	−490			Calvert et al. (2000)
β-pinene + $NO_3 \rightarrow$ Products				2.51×10^{-12}	Calvert et al. (2000)
Camphene + $NO_3 \rightarrow$ Products				6.6×10^{-13}	Calvert et al. (2000)
Myrcene + $NO_3 \rightarrow$ Products				1.1×10^{-11}	Calvert et al. (2000)
Limonene + $NO_3 \rightarrow$ Products				1.22×10^{-11}	Calvert et al. (2000)

[a] Reaction rate constants are reported as: $k(T) = Ae^{-(E_a/R)/T}$, in units of $(\text{cm}^3\,\text{molecule}^{-1}\,\text{s}^{-1})$.
[b] Equilibrium constants are reported as: $K_{eq} = Ae^{B/T}$, in units of $(\text{cm}^3\,\text{molecule}^{-1})$.
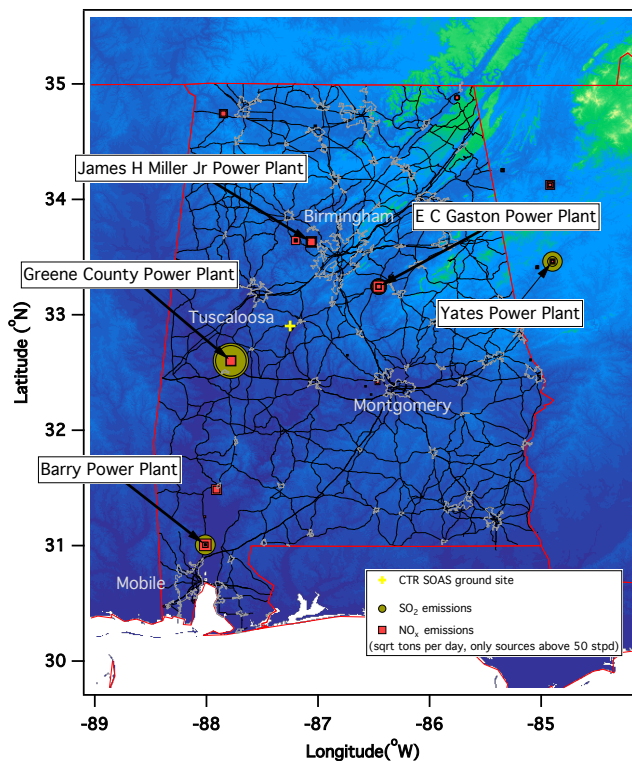
Figure 1. Map of Alabama with SO_2 and NO_x emissions point sources shown, as well as major roadways (black). Centreville is located in Central Alabama about 55 miles SSW of Birmingham, AL. Major highways, city limits and major contributors to emissions are referenced for Alabama. The size of the emission markers depicts the relative concentrations of the pollutants according to the 2013 EPA Air Markets Program. For reference, the Alabama Power Company Gaston Plant emits $19.52\,\mathrm{kg\,h^{-1}}$ SO_2 and $6.43\,\mathrm{kg\,h^{-1}}$ NO_x.
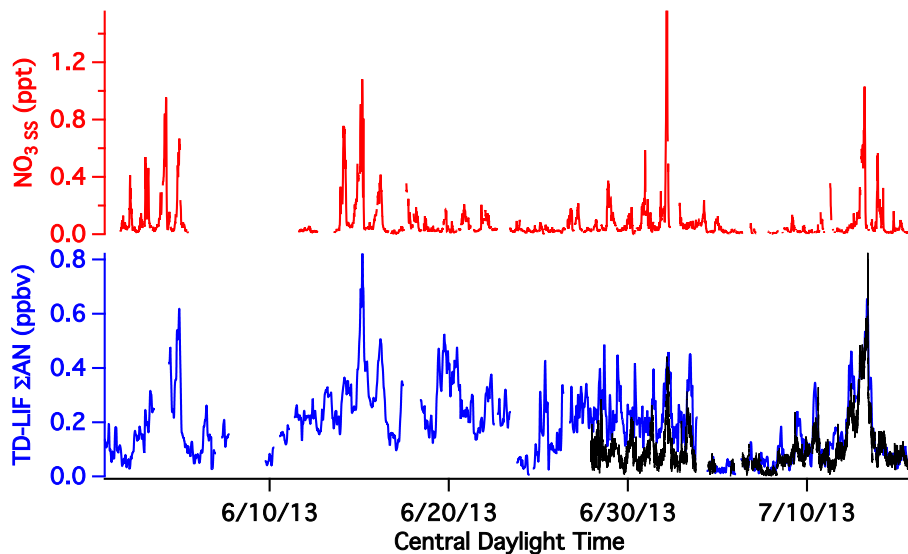
Figure 2. Nitrate radical concentration estimated by the steady-state approximation (red trace) shows several instances where peaks in the small NO_3 concentration correspond to times of ΣAN (gaseous+aerosol) buildup (blue trace). The black overlay is the aerosol phase measurement of ΣANs and qualitatively shows that, when data is available, a large portion of the organic nitrates appear to be in the aerosol-phase.
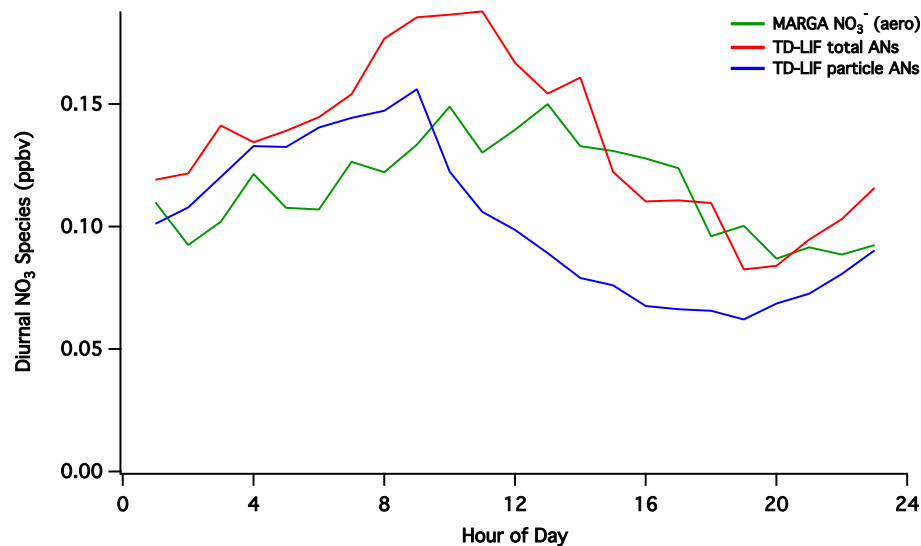
Figure 3. Diurnally averaged organic and inorganic nitrates show organic nitrates peaking in the early morning and inorganic nitrates peaking midday.
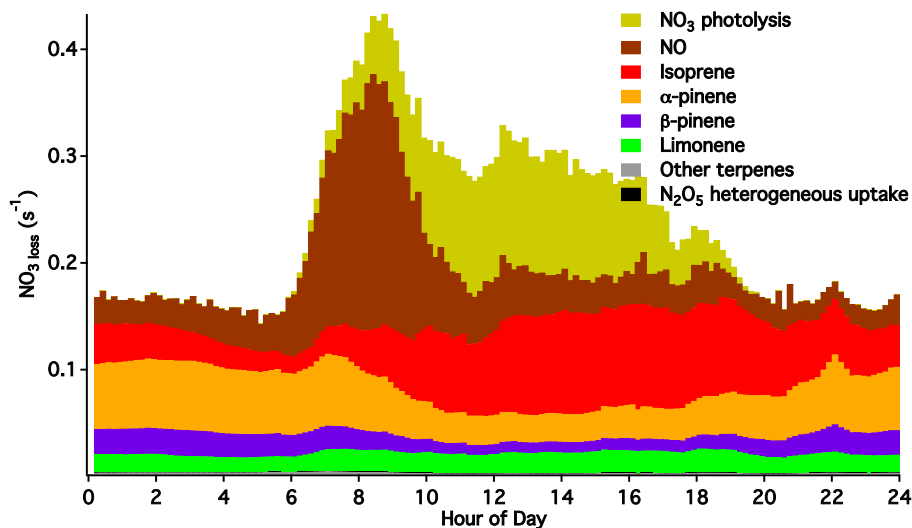
Figure 4. Average diurnal profile of NO_3/N_2O_5 losses 1 June–15 July 2013. NO and photolysis peak during the daytime, however losses to alkenes are significant during both night and day. Terpene losses are calculated from GC-MS data, NO and N_2O_5 data are from CRD, and photolysis losses are calculated as described in Sect. 3.1.
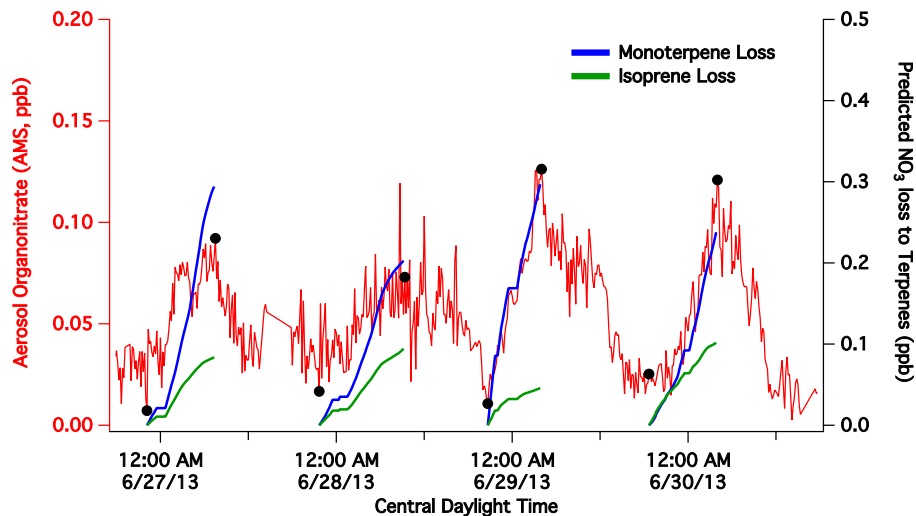
Figure 5. Sample calculation of $(NO_{3,loss})_{integ}$ overlaid against aerosol $RONO_2$ measured by AMS (red). The monoterpene maxima correlate well with the AMS maxima (black dots) The time period shown is arbitrarily chosen.
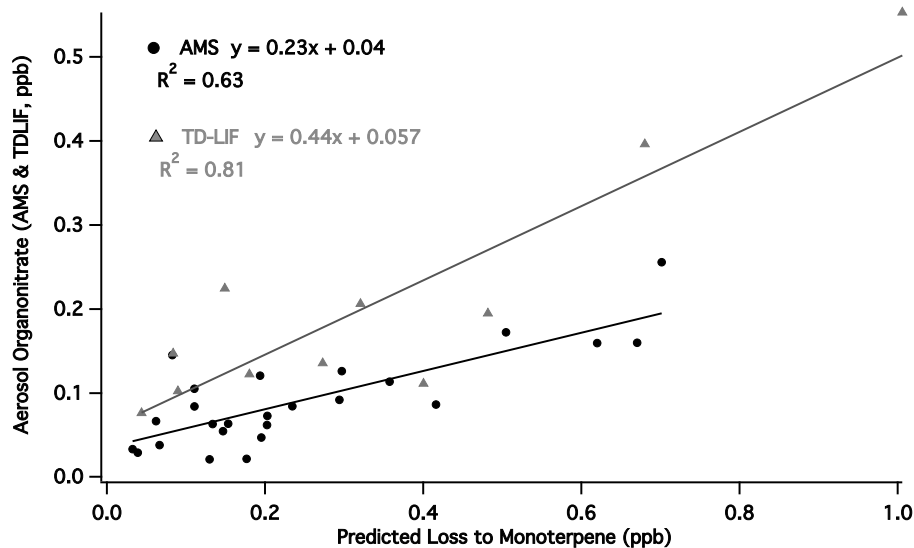
Figure 6. Scatter plots of aerosol RONO$_2$ (AMS and TD-LIF) compared to (NO$_{3,loss}$)$_{cum}$. The magnitudes of the two particle phase organic nitrate measurements differ by a factor of ≈ 2 for unknown reasons, however the slope can be used as a relative molar yield of NO$_3$ loss to monoterpenes. Time period for AMS comparison is 9 June–15 July 2013 and for TD-LIF is 27 June–15 July 2013.
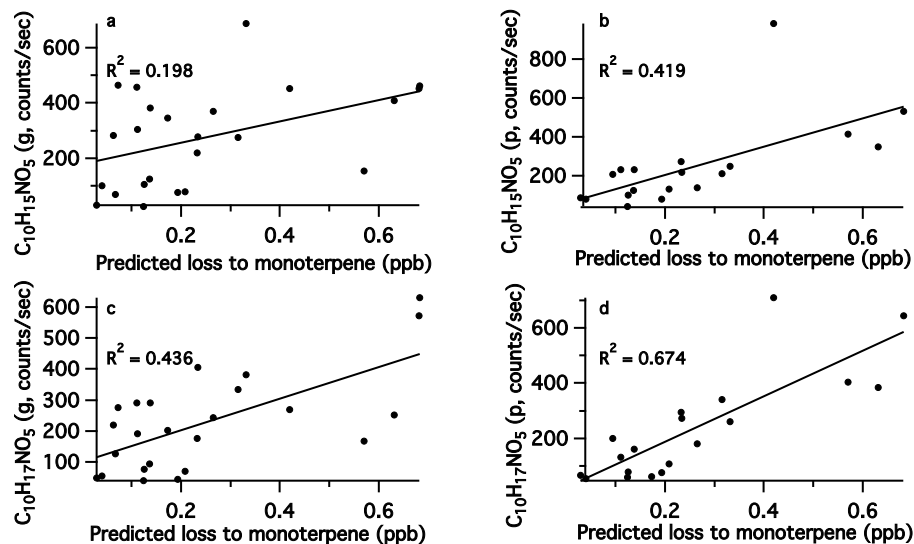
Figure 7. Scatter plots of organic nitrates measured by CIMS against time-integrated monoterpene losses to NO_3 radical. **(a, c)** show gas phase $C_{10}H_{15}NO_5$ and $C_{10}H_{17}NO_5$, respectively. **(b, d)** show particle phase $C_{10}H_{15}NO_5$ and $C_{10}H_{17}NO_5$ respectively. **(d)** gives the best fit with an R^2 value of 0.67 suggesting $C_{10}H_{17}NO_5$ is the best representative NO_3 + monoterpene product that partitions to the aerosol-phase.
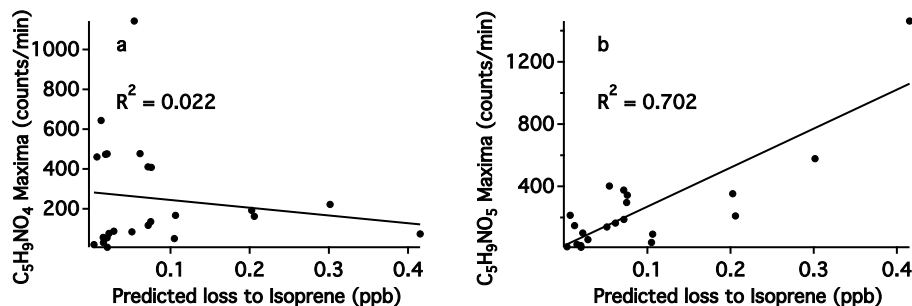
Figure 8. Gas phase CIMS data correlated to predicted isoprene + NO_3 reaction. **(a)** $C_5H_9NO_4$ is poorly correlated to isoprene + NO_3 suggesting that this product comes from another reaction (ex. RO_2+NO). **(b)**, $C_5H_9NO_5$ is well correlated to predicted Isoprene + NO_3 suggesting this is a major gas-phase product.

Full Screen / Esc

Printer-friendly Version
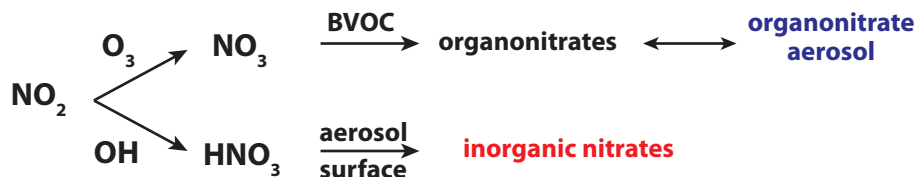
Interactive Discussion
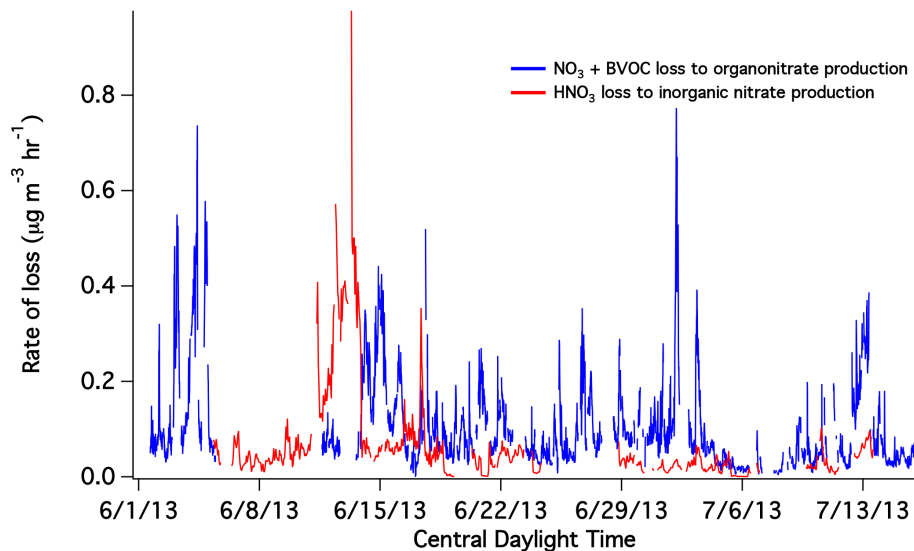
Figure 9. Over the campaign, similar magnitudes of the rate of formation of organic and inorganic nitrate aerosol (according to the pathways shown in Scheme 1) are observed, though peaks occur at different times.

Discussion Paper | Discussion Paper | Discussion Paper | Discussion Paper | Discussion Paper

Scheme 1. Generalized reaction fate for NO_2 in the troposphere. Oxidation of NO_2 from atmospheric oxidants leads to two possible paths.